RSC Advances

ROYAL SOCIETY OF CHEMISTRY

www.rsc.org/advances

Journal Name

ARTICLE

Thienopyrimidine sulphonamide hybrids: Design, synthesis, antiprotozoal activity and molecular docking studies

Received 00th January 20xx,
Accepted 00th January 20xx

DOI: 10.1039/x0xx00000x

www.rsc.org/

Saadia Leeza Zaidi[a], Subhash M Agarwal[b], Porntip Chavalitshewinkoon-Petmitr[c], Thidarat Suksangpleng[c], Kamal Ahmad[d], Fernando Avecilla[e] , Amir Azam[a*]

Abstract: A series of hybrid molecules containing the thienopyrimidine scaffold as DHFR inhibitor fused with the bioactive sulphonamide piperazine skeleton were synthesised and evaluated against chloroquine and pyrimethamine resistant K1 strain of *Plasmodium falciparum* and HM1: 1MSS strain of *Entamoeba histolytica* respectively. Few compounds showed better results than the standard drugs. Toxicity of the hybrids was measured on the Chinese hamster cell line. Majority of the compound had low toxicity. The binding modes of the most potent antimalarial compounds (5, 6 and 8) were also investigated against *Pf*DHFR using molecular docking and enzyme binding studies, in which the result of 5 and 6 were found most promising against *Pf*DHFR. The present studies suggest that these hybrids might be possible antiprotozoal lead molecules for further investigation.

[a]*Department of Chemistry, Jamia Millia Islamia, Jamia Nagar, 110 025, New Delhi, India*
[b] *Bioinformatics Division, Institute of Cytology and Preventive Oncology (ICMR) I-7, Sector-39, Noida 201301, Uttar Pradesh, India*
[c]*Department of Protozoology, Faculty of Tropical Medicine, Mahidol University, Bangkok 10400, Thailand.*

[d]*Centre for Interdisciplinary Research in Basic Science, Jamia Nagar, 110 025, New Delhi, India*

[e]*Departamento de Química Fundamental, Universidade da Coruña, Campus da Zapateira, 15071 A Coruña, Spain.*

*To whom correspondence should be addressed: tel.: +91 11 2698 1717/3254; fax: +91

1. Introduction

The world's population is plagued by numerous parasitic protozoal diseases that are a huge burden to the society. Amoebiasis caused by *Entamoeba histolytica* (*E. histolytica*) a protozoan, leads to a loss of 100,000 lives annually [1]. Effective chemotherapy with the 4-nitroimidazole class of drugs exists but is marred by the fact that it is found to be genotoxic to humans and in addition to this there are reports of development of resistance to the present chemotherapy by the parasite which can cause a major health problem [2-3]. Malaria, another protozoal disease caused by *Plasmodium falciparum* (*P. falciparum*) results in a mortality rate of approximately half a million people all over the world [4]. The scare of the disease is more alarming due to the emergence of chloroquine resistant and multiple drug resistance strain of malaria parasites [5]. This has accelerated the search for hybrid anti-malarial to overcome the problem of drug resistance. Designing hybrid molecules in which two or more pharmacophore are covalently linked to form one molecule is an upcoming field in this direction [6-7]. Such designing allows for synergic action resulting in active moiety and reduction in unwanted side effects [8]. Thienopyrimidines is a highly promising heterocyclic scaffold possessing a diverse range of biological activities such as antituberculosis, anti-inflammatory, anticancer, antiviral, antimalarial [9-13]. The enzyme dihydrofolate reductase (DHFR) a key enzyme in the folate biosynthetic pathway, critical to the biosynthesis of DNA, RNA, and some amino acids is an important target for the development of novel chemotherapeutic agents for malaria, cancer and various microbial diseases. Thieno[2,3-d]pyrimidines have been reported to be DHFR inhibitors [14-16] Literature survey revealed that compounds bearing the piperazine sulphonamide scaffold possess a broad range of pharmacological activities such as anti-HIV, anti-microbial, anti-proliferative, anti-fungal, anti-diabetic, anti-convulsant, anti-TB and anti-protozoal [17-24].

In view of the above properties of thienopyrimidine and piperazine sulphonamide skeleton, the two pharmacophores were covalently linked to generate a single hybrid molecule (Fig.1) and evaluated against HM1: IMSS strain of *E.histolytica* and K1 strain of *P.falciparum* in anticipation that the hybrid molecules will show potent anti-protozoal activity due to the synergistic effect of the two scaffolds. The *in vitro* results of the hybrids were further validated by molecular docking and enzyme binding studies on *Pf*DHFR.

2. Results and Discussion

2.1. Chemistry

The 4-Piperazine-1-yl-5,6,7,8-tetrahydrobenzothiopheno[2,3-d] pyrimidine based sulphonamides was synthesized by a reported method [24]. Cyclohexanone was condensed with ethyl cyanoacetate under basic condition and then cyclized in the presence of sulfur to construct the thiophene core (1) through Gewald reaction as given in scheme 1. Cyclization with formamide gave the basic thieno pyrimidine core (2) which on reaction with $POCl_3$ gave the 4-chloro-5,6,7,8 tetrahydrobenzothiopheno[2,3-d]pyrimidine (3). Piperazine was reacted with 4-chloro-5,6,7,8 tetrahydrobenzothiopheno[2,3-d]pyrimidine in ethanol resulted the formation of intermediate 4-piperazine-1-yl-5,6,7,8-tetrahydrobenzothiopheno[2,3-d] pyrimidine (4) [25]. The reaction proceeds via aromatic nucleophilic substitution. The thienopyrimidine sulphonamide hybrids (5-14) were synthesized by the reaction of 4-piperazine-1-yl-5,6,7,8 tetrahydrobenzothiopheno [2,3-d] pyrimidine (4) with different substituted sulphonyl chlorides in dichloromethane. Triethylamine was used as a base at 0^{o}C to room temperature (scheme 1.). The compounds were recrystallized from dichloromethane and methanol (1:9).

2.2. Biology

2.2.1. Antiamoebic Activity

The antiamoebic potential of the hybrid molecules was tested on the HM1: IMSS strain of *E. histolytica* by microdilution method. The antiamoebic activity was compared with the standard amoebicidal drug metronidazole (MNZ) that had 50% inhibitory concentration (IC_{50}) 1.86±0.02μM. The results manifested that the intermediate 4 had IC_{50} value 3.29±0.02 μM which suggests that the intermediate is less potent than the standard drug MNZ. Further reaction of the intermediate with different substituted sulphonyl chlorides yielded compounds exhibiting a range of IC_{50} values (0.35±0.03 - 5.8±0.02 μM) shown in Table 1. The structure activity relationship (SAR) of compounds 10 and 12 (IC_{50} 0.78±0.02 μM and 0.35±0.03 μM) bearing electron donating group was found twofold increase in activity better inhibitors of *E. histolytica* than MNZ. The presence of aliphatic substitution compounds 9 and 11 (IC_{50} 1.36±0.01 μM and 1.70±0.01μM) lead to the enhancement in the antiamoebic potency. The enhancement in the activity observed on moving from methyl to propyl substituted sulphonamides may be attributed to the elongation of alkyl chain. Further, it was observed that introduction of electron withdrawing group as in compounds 7 (IC_{50} 3.0±0.02 μM), 8 (2.82±0.02 μM) and 14 (IC_{50} 2.02±0.02 μM) or bulky groups as in the compounds 5 (5.8±0.02 μM) and 6 (IC_{50} 4.6±0.02 μM) had a negative effect on the activity.

2.2.2. Antimalarial Activity

All the synthesised compounds were evaluated for their inhibitory effects on *P. falciparum* K1 growth by *in vitro* assay. The inhibitory effects of compounds are presented in Table 1. Based on the results, all compounds showed parasite growth inhibition with different IC_{50} ranging from <0.1 - 18.5±0.03 μM. IC_{50} of the intermediate 4 and final compound 13 were 2.07±0.01 and 3.15±0.02 μM respectively. The most potent compounds against *P. falciparum* in culture were 5 and 8 (> 0.1 μM) with IC_{50} less than that of chloroquine. The antimalarial potency of compound 7 and 14 (IC_{50} 7.85±0.02 μM and 18.5±0.03 μM respectively) was found very low as compared to chloroquine. According to structure activity relationship, compound 5 containing t-butyl group at *para* position was most active while compound 7 containing *ortho* NO_2 group and 14 containing Cl group at *para* position of benzene ring showed low inhibition on parasite growth. However, compound 6 containing naphthalene group as substitution at this *para* position was found to be active with IC_{50} 0.1±0.001 μM and its antimalarial activity is similar to that of the reference drug chloroquine. Compound 8 containing two chloro group at position 2 and 5 inhibited *P. falciparum* growth (IC50 < 0.1 μM) at low concentration. Compounds 9 and 11 having aliphatic sulphonamide substitution showed fairly good activity with IC_{50} 1.02±0.01 μM and 0.9±0.001 μM respectively. In addition, compounds 10 and 12 having electron donating group also gave nearly the same IC_{50} of 1.98±0.01 μM and 1.94±0.02 μM respectively. The variation in IC_{50} obtained for antimalarial and antiamoebic activities of some compounds may be due to different uptake capability of these parasites or availability of drug targets in their cells.

2.2.3. Cytotoxic Activity

The IC_{50} of compounds (5, 6, 8, 9, 10, 11 and 12) could not be determined although the concentration was raised up to 50 μM (Table 1). Cytotoxicity of compounds was assessed by MTT assay on Chinese hamster ovary (CHO) normal cell line. A confluent population of CHO cells was treated with increasing concentrations of compounds and the number of viable cells was measured after 48 h by MTT-cell viability assay based on mitochondrial reduction of the yellow MTT tetrazolium dye to a highly coloured blue formazan product. This assay usually shows high correlation with number of live cells and cell proliferation. The concentration range for all the compounds (5, 6, 8, 9, 10, 11, 12, MNZ and CQ) are mentioned in Fig-5, which illustrates that all the active compounds and standard compounds were low-cytotoxic in the

concentration range of 1.56-25 µM for 48 h. At 50 µM for 48 h, only three compounds, 5, 6 and 8 showed maximum viability and least cytotoxicity. Therefore, it can be concluded that the cytotoxicity of all the compounds (5, 6, 8, 9, 10, 11 and 12) was found to be concentration-dependent and all the screened compounds were least cytotoxic against the Chinese hamster ovary (CHO) normal cell line in the concentration range of 1.56-25 µM.

2.3. Pharmacokinetics

Most of the drugs fail in clinical trials due to weak pharmacokinetic properties and cellular toxicity. Therefore, *in silico* pharmacokinetic profile of selected compounds was evaluated to fetch the putative bioavailability for *Pf*DHFR inhibitors (Table 2). Physicochemical properties, especially aqueous solubility (logS), lipophilicity (clogP), polar surface area (PSA), and molecular weight (MW) are directly related to the absorption and bioavailability of a drug molecule [26]. These properties directly affect the movement of a drug from the site of administration into the blood. The CYPs (cytochrome P450) play a significant role in drug metabolism and are equally important for disposition of drugs in body, their pharmacological and toxicological effects [27].

The ADMET (DS3.5) was used to get the probable pharmacokinetic profile of molecules. It utilises QSAR models to compute the ADMET related properties for small molecules. Alog P value (Lipophilicity) is significant property for the prediction of per oral bioavailability of drug molecules [28]. Results showed that synthesized compounds 6 have ideal Alog P value ≤ 5, except synthesized compounds like 5 and 8 (logP=4.856). However, logP value up to 6 is considerable for a drug molecule [29]. Similarly, all selected synthesised compounds showed moderate to good range of solubility level (solubility level= 0 to 4). The best synthesize compound 6 showed better solubility with level 1, AlogP=4.856, having good absorption level 0 and good hepatotoxicity level, i.e., 0. All compounds (5, 6 and 8) showed hepatotoxicity probability score ≤ 0.5. The observed human intestinal absorption (HIA) value is excellent for all molecules. The blood-brain-barrier (BBB) penetration ability of compounds is high when prediction value is zero and is least for the prediction value of 4. All synthesized molecules showed better ability for blood-brain-barrier (BBB=0-4).

The antiprotozoal drug chloroquine having a good ADMET profile (logP= 0.029, BBB=3, solubility = 4 and HIA=0), showed less hypotoxicity effect and is also not reactive to CYP2D6. The CYP2D6 probability of all synthesized compounds showed<0.5, demonstrated that all compounds were non-inhibitor to CYP2D6 enzyme. For good druggability, the ideal plasma protein binding (PPB) level is 0. All synthesized compounds with chloroquine showed better PPB activity. PSA is dependent on the conformation and hydrogen-bonding. It implies the single low-energy conformer of the molecule. For activity of a drug, the optimum value of PSA is ≤ 90 Å [30]. The hydrogen bonding and logP value are the two important descriptors to define the PSA of drug molecule. All predicted compounds showed significant PSA.

The computer-aided toxicity predictor, TOPKAT was used to examine the cellular toxicity of synthesize compounds. The carcinogenic and mutagenic effect of compounds with WOE Prediction (weight of evidence) and Ames Prediction was our primary goal. It comprises of various models and toxicity endpoints (irritation, teratogenicity, sensitization, neuro-toxicity and immunotoxicology) that are often employed in drug development. All the selected compounds with known inhibitor showed Ames probability score ≤ 7 and are non-mutagen. Other toxicity predictor WOE (weight of evidence) was employed to examine the relative level of certainty of compounds that may cause cancer in humans. All compounds were found to be noncarcinogenic, except known inhibitor is predicted. The ADMET score and TOPKAT property data of virtual synthesized compounds with standard drug, suggested that selected molecules may be exploited as bioactive compounds.

2.4 Molecular Docking

The binding mode of active thienopyrimidine based sulphonamide anti-malarial compounds (5, 6, 8) has been determined to understand the protein-ligand contacts and their interaction strength, these compounds were docked in the active site of crystal structure of *Pf*DHFR using AutoDock. Initially WR99210, the co-crystallised compound in the active site of wild *Pf*DHFR was docked and observed that the root-mean-square deviation (RMSD) between the original and re-scored docked ligand was 1.19 Å validating the docking protocol. The compounds 5, 6 and 8 were then docked and observed that they fit into the active pocket of *Pf*DHFR with binding energy of -9.84 kcal/mol, -9.95 kcal/mol and -9.59 kcal/mol respectively. The thienopyrimidine based sulphonamide compounds exhibited similar pose as that of co-crystallised ligand WR99210 in the binding region (Fig. 6). The 2D interaction plots indicated that the three ligands (5, 6 and 8) also exhibit H-bonding with Ile164 as observed in WR99210. Also, these compounds showed conserved hydrophobic interactions with the active site residues Ile14, Cys15, Ala16, Val45, Leu46, Lys49, Asp54, Met55, Phe58, Ser111, Ile112 and Tyr170. The molecular docking thereby supports the data that such sulphonamide analogues could act as antiprotozoal agents by inhibiting *P. falciparum* DHFR.

2.5. PfDHFR marker interaction with ligands:

The results revealed that interaction of *Pf*DHFR protein with standard compound (CQ) bind to active site region and change the conformation of protein that create dilemma between protein and compound in experiment-1 (Figure 7 A) while in other set of experiment-2 showed that the interactions of *Pf*DHFR protein with DNA substrate (DNA oligo labelled with Y^{32}ATP hot), conformation of protein did not change from native form. Therefore, the substrate binds to few region of the protein due to this low signal was visualised in the autoradiogram (Figure 7B). In all the experiments BSA is the negative control (C) and chloroquine (CQ) was used as a positive control (Figure 7 A and 7 B). In test experiments the result clearly showed binding affinity of *Pf*DHFR marker protein at various concentrations (2.5-100µM) of the compounds. The results revealed that at lower concentration of compounds the conformation of protein does not change. Hence, the substrate binds to its own region and more signals were visualised. When concentration of the compounds was increased from 50 µM to 100µM then the binding region of DNA oligo was covered resulting in low signals, which means interaction of compounds and proteins was significant (Figure 7C, compound 5, a-b and compound 6, c-d). In case of compound 8 there was no change in protein conformation even on increasing the concentration of compound. The substrate showed the constant signal as the protein did not bind to compound significantly (Figure 7C, compound 8, e-f). Hence compounds 5 and 6 may have better binding affinity towards *Pf*DHFR than compound 8.

3. Experimental

All the required chemicals were purchased from Merck and Aldrich Chemical Company (USA). Precoated aluminium sheets (silicagel 60 F_{254}, Merck Germany) were used for thin- layer chromatography (TLC) and spots were visualized under UV light. Elemental analysis was carried out on CHNS Elementar (Vario EL-III, Germany) and the results were within ±0.3% 0f

the theoretical values. IR spectra were recorded on Bruker FTIR spectrophotometer. ^{1}H NMR and ^{13}C NMR spectra were recorded on Bruker Spectrospin DPX 300 MHz using $CDCl_3$ or DMSO as a solvent and trimethylsilane as an internal standard. Splitting patterns are designated as follows: s, singlet; d, doublet; m, multiplet. Chemical shift values were given in ppm. The FAB mass spectra of the compounds were recorded on JEOL SX 102/DA-6000 mass spectrometer using Argon/Xenon (6 KV, 10 Ma) as the FAB gas and m-nitrobenzyl alcohol (NBA) was used in the matrix.

3.1. Synthesis of intermediate (4):

To a stirred solution of 4-chloro-5,6,7,8 tetrahydrobenzothiopheno [2,3-d]pyrimidine (44 mmol) in 150 mL ethanol was added piperazine (156 mmol). The resulting solution was refluxed for 12 h. The completion of reaction was monitored on TLC and concentrated under *vacuo* gave a crude solid mixture which was then taken in 250 mL of dichloromethane and washed with saturated sodium bicarbonate solution until no piperazine was seen in the organic layer (TLC). The combined organic extracts were dried over anhydrous sodium sulphate, concentrated and recrystallized from dichloromethane.

3.1.1. 4-Piperazin-1-yl-5,6,7,8-tetrahydrobenzo [4,5]theino[2,3-d] pyrimidine (4)**:** Yield 70 % ; m.p. 280˚C ; Molecular formula: $C_{14}H_{18}N_4S$; Elemental analysis Calculated : C 61.28% , H 6.61% , N 20.42% ,S 11.69% ; found C 61.24% , H 6.60% , N 20.44% , S 11.67% ; FT-IR ν_{max} (cm^{-1}): 3240 (NH), 1531 (C=N), 972 (C-N); ^{1}HNMR (300 MHz,$CDCl_3$) δ(ppm) :8.54 (s, 1H, pyrimidine), 4.36 (s, 1H, NH), 3.66-3.59 (m, 2H) , 3.43-3.30 (m, 2H), 2.89 (s, 4H) 2.72 (s, 2H), 1.94-1.82 (m, 4H) ; ^{13}CNMR($CDCl_3$) δ(ppm): 168.27, 162.46, 151.49, 135.12, 127.23, 121.44, 51.90, 45.66, 26.76, 25.81, 23.00, 22.83; ESI-MS: m/z = 275 [M+1].

3.2.General procedure for the synthesis of 4-[4-Aryl/ Alkyl sulphonyl)-piperazine-1-yl]-5,6,7,8-tetrahydrobennzo[4,5]theino[2,3-d] pyrimidine (5-14)**:** To a stirred solution of 4-Piperazin-1-yl-5,6,7,8-tetrahydrobenzo [4,5]theino[2,3-d] pyrimidine (1.81 mmol) in 10 ml dichloromethane at 0˚C was added triethylamine (1.81mmol) and different substituted sulfonyl chlorides (1 mmol) for 5-8 h. The reaction was monitored by TLC. The reaction mixture was poured on water and extracted from dichloromethane. The crude solid was re-crystallized from dichloromethane and methanol.

3.2.1. **4-[4-(4-tert-Butylbenzenesulphonyl)-piperazine-1-yl]-5,6,7,8-tetrahydrobenzo [4,5]theino [2,3-d] pyrimidine (5):** yield 88%; m.p. 161˚C; Molecular formula $C_{21}H_{24}N_4O_2S$; Elemental analysis Calculated: C 58.85% ,H 5.64% ,N 13.07% ,S 14.96% found: 58.89% , H 5.671%, N 13.11% ,S 14.89%; FT-IR ν_{max} (cm^{-1}): 1533 (C=N),1340, 1164 (SO2), 960 (CN); ^{1}HNMR (300 MHz,$CDCl_3$) δ (ppm): 8.47 (s, 1H, pyrimidine), 7.734 (d, 2H, *J* = 8.4Hz, ArH), 7.58 (d, 2H, *J*=8.4Hz, ArH), 3.55 (t, 4H, *J*=4.5Hz, CH_2N), 3.22 (t, 4H, *J*=4.5 Hz, CH_2N), 2.88 (t, 4H, *J*=6.0Hz, CH2), 1.93-1.91 (m, 2H, CH_2), 1.77-1.63 (m, 2H, CH_2); 1.36 (s, 9H, C(CH_3)$_3$); ^{13}CNMR ($CDCl_3$) δ (ppm): 161.40, 156.81, 151.30, 135.76, 133.11, 127.63, 127.70, 126.14, 121.21, 49.94, 45.37, 35.19, 31.06, 26.61, 25.77, 22.91, 22.75; ESI-MS: m/z = 471 [M+1].

3.2.2 4-[4-(Napthalene-1-sulphonyl) –piperazine-1-yl]-5,6,7,8-tetrahydrobenzo[4,5] theino [2,3-d] pyrimidine (6)**:** Yeild 85%; m.p. 185˚C; Molecular formula $C_{24}H_{24}N_4O_2S_2$;Elemental analysis Calculated: C 62.04%, H 5.21%, N 12.06%, S 13.80% Found: C 62.10%, N 12.07%, H 5.03%, S 13.56%; FT-IR ν_{max} (cm^{-1}): 3045 (C=C), 1528 (C=N), 1129, 1075 (SO_2), 960 (CN); ^{1}HNMR (300MHz, $CDCl_3$) δ (ppm): 8.459 (s, 1H, pyrimidine), 8.39 (s, 1H, ArH), 8.037-7.953 (m, 3H, ArH), 7.80-7.70 (m, 1H), 7.68-7.28 (m, 2H, ArH), 3.55 (t, 4H, J=5.6Hz, CH_2N), 3.29 (t, 4H, J=6.9Hz, CH_2), 2.86 (m, 4H, CH_2), 1.91-1.88 (m, 2H), 1.79-1.72 (m, 2H); ^{13}C NMR ($CDCl_3$) δ (ppm): 161.41, 151.32, 135.82, 134.99, 133.28, 132.27, 129.45, 129.27, 129.15, 128.97, 127.99, 127.67, 126.65, 122.86, 50.01, 45.49, 26.56, 25.77, 22.87, 22.72; ESI-MS: m/z = 465 [M+1].

***3.2.3. 4-[4-(2-Nitro-1-sulphonyl)-piperazine-1-yl]-5,6,7,8 tetrahydrobenzo[4,5]theino [2,3-d] pyrimidine (7)*:** Yield 75%; m.p. 155°C; Molecular formula $C_{20}H_{21}N_5O_4S_2$; Elemental analysis Calculated: C 52.27%, H 4.61%, N 15.24%, S 13.95% found: C 52.53%, H 4.665%, N 15.37%, S 13.76%; FT-IR ν_{max} (cm^{-1}): 1538 (C=N), 1435, 1317 (NO_2), 1360, 1072 (SO_2); ^{1}HNMR (300MHz, $CDCl_3$) δ (ppm): 8.52 (s, 1H, pyrimidine), 8.04-7.99 (m, 1H, ArH), 7.74-7.68 (m, 3H, ArH), 3.52 (s, 8H, CH_2N), 2.89 (s, 4H), 1.95-1.80 (m, 4H); ^{13}CNMR ($CDCl_3$) δ (ppm): 168.66, 161.55, 151.33, 148.35, 135.99, 133.93, 131.74, 131.46, 130.99, 126.71, 124.25, 121.44, 50.24, 45.38, 26.59, 25.79, 22.90, 22.72; ESI-MS: m/z = 460 [M+1].

3.2.4. 4-[4-(2,5-Dichloro-benzenesulphonyl)-piperazine-1-yl]-5,6,7,8 tetrahydrobenzo [4,5] theino [2,3-d] pyrimidine (8): Yield 84%; m.p. 160°C; Molecular formula $C_{20}H_{20}Cl_2N_4O_2S_2$; Elemental analysis Calculated: C 52.27%, H 4.61%, N 15.24%, S 13.95%, found: C 52.53%, H 4.66%, N 15.37%, S 13.88%; FT-IR ν_{max} (cm^{-1}): 1533 (C=N), 1366, 1128 (SO_2), 962, (CN), 707 (C-Cl); ^{1}HNMR (300MHz, $CDCl_3$) δ (ppm): 8.534 (s, 1H, pyrimidine), 8.10 (s, 1H, ArH), 7.49 (s, 2H, ArH), 3.55-3.41 (t, 8H, *J*=5.7Hz, CH_2N), 2.90-2.88 (d, 4H, *J*=5.1, CH_2), 1.95-1.83 (m, 4H, CH_2); ^{13}C NMR ($CDCl_3$) δ (ppm): 168.61, 161.33, 151.26, 139.65, 135.995, 134.61, 129.56, 129.07, 126.60, 121.27, 49.89, 45.37, 26.53, 25.75, 22.88, 22.69; ESI-MS: m/z = 484 [M+1].

***3.2.5. 4-[4-(Propane- 1- sulphonyl)- piperazine-1-yl] – 5,6,7,8- tetrahydrobenzo [4,5] theino [2,3-d] pyrimidine (9)*:** Yield 86%; m.p. 155°C; Molecular formula $C_{17}H_{24}N_4O_2S_2$; Elemental analysis calculated: C 53.38%, N 14.65%, H 6.85%, S 16.76% Found: C 54.17 %, N 14.70%, H 6.88%, S 16.66%; FT-IR ν_{max} (cm^{-1}): 1533 (C=N), 1318 , 1138 (SO_2), 945 (CN);^{1}HNMR (300 MHz, $CDCl_3$) δ (ppm): 8.55 (s, 1H, pyrimidine), 3.69-3.50 (m, 8H, CH_2N), 2.97-2.84 (m, 6H), 1.97-1.84 (m, 6H), 1.12 (t, 3H, *J*=7.5Hz, CH_3); ^{13}CNMR ($CDCl_3$) δ (ppm): 168.59, 161.64, 150.70, 136.00, 126.73, 121.48, 52.24, 49.35, 45.23, 26.64, 25.82, 22.91, 16.86, 13.83; ESI-MS: m/z = 381 [M+1].

***3.2.6. N-{4-[4-(5,6,7,8-Tetrahydrobenzo [4,5] theino [2,3-d] pyrimidin-4-yl) –piperazine-1- sulphonyl]-phenyl}-acetamide (10)*:** Yield 88%; m.p. 380°C; Molecular formula $C_{22}H_{25}N_5O_3S_2$; Elemental analysis Calculated: C 56.03%, H 5.34%, N 14.85%, S 13.60% found: C 56.50%, H 5.21%, N 14.80%, S 13.70%; FT-IR ν_{max} (cm^{-1}): 3353 (NH), 1661 (C=O), 1529 (C=N), 1131, 1158 (SO_2), 936 (CN); ^{1}HNMR (300MHz, $CDCl_3$) δ (ppm): 8.46 (s, 1H, pyrimidine), 7.73 (d, *J*= 9.0 Hz, 2H, ArH)), 7.02 (d, *J*=9.0 Hz, 2H, ArH), 3.88 (s, 3H), 3.54-3.50 (m, 4H), 3.48-3.45 (m, 4H), 2.88-2.77 (m, 4H), 1.96-1.67 (m, 4H); ^{13}CNMR ($CDCl_3$) δ (ppm): 163.34, 157.95, 156.15, 146.04, 130.49, 124.60, 122.24, 121.46, 115.96, 109.12, 50.38, 44.64, 40.17, 21.32, 20.52, 17.66, 17.47; ESI-MS: m/z = 472 [M+1].

***3.2.7. 4-(4-Methane sulphonyl piperazin-1-yl) - 5,6,7,8 – tetrahydro – benzo [4,5] theino [2,3 – d] pyrimidine (11)*:** Yield 88%; m.p. 150°C; Molecular formula $C_{15}H_{20}N_4O_2S_2$; Elemental analysis Calculated: C 51.11%, H 5.77%, N 15.90%, S 18.19%, found: C 51.03%, H 5.77%, N 15.88%, S 18.18%; FT-IR ν_{max} (cm^{-1}): 1526 (C=N), 1355,1150 (SO_2), 938 (CN); ^{1}HNMR (300 MHz, $CDCl_3$) δ (ppm): 8.55 (s, 1H, pyrimidine), 3.57- 3.54 (m, 4H, CH_2N), 3.42 – 3.14 (m, 4H, CH_2N), 2.91–2.88 (m, 4H, CH_2N), 2.86 (s, 3H, CH_3), 1.96 – 1.84 (m, 4H, CH_2); ^{13}CNMR ($CDCl_3$) δ (ppm): 168.71, 161.54, 151.39, 136.04, 126.67, 121.46, 50.16, 45.28, 34.91, 26.63, 25.81, 22.93, 22.75; ESI-MS: m/z = 353 [M+1].

***3.2.8 4-[4-(4-Methoxy-benzenesulphonyl) – piperazine – 1 –yl] -5,6,7,8 –tetra hydro-benzo [4,5] theino [2,3 –d] pyrimidine (12)*:** Yield 90%; m.p. 180°C; Molecular formula $C_{21}H_{24}N_4O_2S_2$; Elemental analysis Calculated: C 56.74%, H 5.44%, N 12.60%, S 14.42%, found: C 56.76%, H 5.77%, N 12.74%, S 14.27%; FT-IR ν_{max} (cm^{-1}): 1529 (C=N), 1345,1145 (SO_2), 936 (CN); ^{1}HNMR (400MHz, $CDCl_3$) δ (ppm): 8.48 (s, 1H, pyrimidine), 7.74 (d, 2H, *J*=6.6 Hz, ArH), 7.04 (d, 2H, *J*=6.9 Hz, ArH), 3.90 (s, 3H, OCH_3), 3.60 (t, 4H, *J*=4.4 Hz, CH_2N), 3.20 (t, 4H, *J*=4.4 Hz, CH_2N), 2.91 (t, 2H, *J*=6.0 Hz, CH_2), 2.82 (t, 2H, *J*=5.4 Hz, CH_2), 1.97-1.81 (m, 2H, CH_2), 1.81-1.76 (m, 2H, CH_2); ^{13}CNMR ($CDCl_3$) δ (ppm): 169.64, 165.76, 161.13, 150.44, 144.15, 140.05, 135.29, 129.22, 127.73, 120.43, 55.38 ,49.76, 45.87, 26.49, 25.60, 24.48, 22.86, 22.56; ESI-MS: m/z = 445 [M+1].

***3.2.9. 4-[4-Benzenesulphonyl) – piperazine – 1 –yl] -5,6,7,8 –tetrahydro-benzo [4,5] theino [2,3 –d] pyrimidine (13)*:** Yield 83%; m.p. 200°C; Molecular formula $C_{21}H_{26}N_4O_2S_2$; Elemental analysis Calculated: C 57.95%, H 5.35%, N 13.52%, S 15.47%, found: C 57.87%, H 5.40%, N 13.45%, S 15.32%; FT-IR ν_{max} (cm^{-1}): 3340 (C=C), 1532 (C=N), 1351, 1165 (SO_2), 940 (CN); ^{1}HNMR (300MHz, $CDCl_3$) δ (ppm): 8.46 (s, 1H, pyrimidine), 7.80 (d, 2H, *J*=7.2 Hz, ArH), 7.66-7.54 (m, 3H, ArH), 3.52-3.51 (m, 4H, CH_2N), 3.21-3.20 (m, 4H, CH_2N), 2.86-2.78 (m, 4H, CH_2), 1.92-1.90 (m, 2H, CH_2), 1.76-1.75 (m, 2H, CH_2); ^{13}CNMR ($CDCl_3$) δ (ppm): 168.36, 161.34, 151.14, 135.91, 135.84, 133.12, 129.24, 127.71, 126.68, 121.21, 49.90, 45.45, 26.58, 25.78, 22.89, 22.71; ESI-MS: m/z = 415 [M+1].

***3.2.10. 4-[4-(4-Chlorobenzenesulphonyl) – piperazine – 1 –yl] -5,6,7,8 –tetrahydro-benzo [4,5] theino [2,3 –d] pyrimidine (14)*:** Yield 81%; m.p. 206°C; Molecular formula $C_{21}H_{25}N_4O_2S_2Cl$; Elemental analysis Calculated: C 53.50%, N 12.48%, H 4.71%, S 4.28%; found: C 53.05%, N 12.42%, H 4.75%, S 4.40%; FT-IR ν_{max} (cm^{-1}): 1529 (C=N), 1340, 1164 (SO_2), 960 (CN), 822 (CCl); ^{1}HNMR (300MHz, $CDCl_3$) δ (ppm): 8.49 (s, 1H, pyrimidine), 7.75 (d, 2H, *J*=8.4 Hz, ArH), 7.56 (d, 2H, *J*=8.4 Hz, ArH), 3.55-3.52 (m, 4H, CH_2N), 3.22 -3.21 (m, 4H, CH_2), 2.88-2.80 (m, 4H, CH_2), 1.94-1.92 (m, 2H, CH_2), 1.79-1.78 (m, 2H, CH_2); ^{13}CNMR ($CDCl_3$) δ (ppm): 168.70, 161.63, 151.41, 137.79, 136.05, 133.71, 133.32, 133.26, 131.79, 130.51, 126.66, 121.50, 50.41, 45.22, 26.62, 25.81, 22.91, 22.75; ESI-MS: m/z = 450 [M+1].

4. X-Ray crystal structure determination

Three-dimensional X-ray data were collected on a Bruker Kappa Apex CCD diffractometer at low temperature for 9 and 13 by the ϕ-ωscan method. Reflections were measured from a hemisphere of data collected from frames, each of them covering 0.3º inω. 18298 for 9 and 90862 for 13 reflections measured were corrected for Lorentz and polarization effects and for absorption by multi-scan methods based on symmetry-equivalent and repeated reflections. Of them, 3348 and 4187 independent reflections, respectively, exceeded the significance level ($|F|/\sigma|F|$) > 4.0. After data collection, in each case multi-scan absorption correction (SADABS) [31] was applied, and the structures were solved by direct methods and refined by full matrix least-squares on F^2 data using SHELX suite of programs [32]. In 9, hydrogen atoms were left to refine freely, except for C(15A), C(16A), C(17A), C(15B), C(16B) and C(17B), which were included in calculated positions and refined in the riding mode. In 13, hydrogen atoms were left to refine freely. Refinements were done with allowance for thermal anisotropy of all non-hydrogen atoms. A final difference Fourier map showed no residual density in the crystals: 0.427 and -0.329 e.Å^{-3} for 9 and 0.349 and -0.474 e.Å^{-3} for 13. A weighting scheme w = $1/[\sigma^2(F_o^2) + (0.056500\ P)^2 + 0.805900\ P]$ for 9 and w = $1/[\sigma^2(F_o^2) + (0.044100\ P)^2 + 4.008800\ P]$ for 13, where P = $(|F_o|^2 + 2|F_c|^2)/3$, were used in the latter stages of refinement. Crystal of 9 presents a disorder on the propane-1- sulphonyl group. The disorder was resolved and the atomic sites have been observed and refined with anisotropic atomic displacement parameters. The site occupancy factor was 0.72116 for C(15A), C(16A) and C(17A).Further details of the crystal structure determination are given in SA 1.

CCDC 1410920 for 9 and 1410921 for 13 contains the supplementary crystallographic data for the structure reported in this paper. These data can be obtained free of charge via http://www.ccdc.cam.ac.uk/conts/retrieving.html, or from the Cambridge Crystallographic Data Centre, 12 Union Road, Cambridge CB2 1EZ, UK; fax: (+44) 1223 336 033; or e-mail: deposit@ccdc.cam.ac.uk.

5. Pharmacological Evaluation

5.1. Antiamoebic activity

Compounds 4-14 were screened *in vitro* for antiamoebic activity against HM1: IMSS strain of *E. histolytica* by microdilution method [33]. *E. histolytica* trophozoites were cultured in culture tubes by using Diamond TYIS-33 growth

medium [34]. The test compounds (1mg) were dissolved in DMSO (40 µL), level at which level no inhibition of amoeba occurs) [35-36]. The stock solutions of the compounds were prepared freshly before use at a concentration of 1 mg/mL. Two-fold serial dilutions were made in the wells of 96-well microtiter plate (costar). Each test includes metronidazole as a standard amoebicidal drug, control wells (culture medium plus amoebae) and a blank (culture medium only). All the experiments were carried out in triplicate at each concentration level and repeated thrice. The amoeba suspension was prepared from a confluent culture by pouring off the medium at 37 °C and adding 5 mL of fresh medium, chilling the culture tube on ice to detach the organisms from the side of flask. The number of amoeba/mL was estimated with the help of a haemocytometer, using trypan blue exclusion to confirm the viability. The suspension was diluted to 10^5 organism/ml by adding fresh medium and 170 µL of this suspension was added to the test and control wells in the plate so that the wells were completely filled (total volume, 340 µL). An inoculum of 1.7 x 10^4 organisms/well was chosen so that confluent, but not excessive growth, took place in control wells. Plate was sealed and gassed for 10 min with nitrogen before incubation at 37 °C for 72 h. After incubation, the growth of amoeba in the plate was checked with a low power microscope. The culture medium was removed by inverting the plate and shaking gently. Plate was then immediately washed with sodium chloride solution (0.9%) at 37 °C. This procedure was completed quickly and the plate was not allowed to cool in order to prevent the detachment of amoeba. The plate was allowed to dry at room temperature and the amoebae were fixed with methanol and when dried, stained with (0.5%) aqueous eosin for 15 min. The stained plate was washed once with tap water, then twice with distilled water and then allowed to dry. 200 µL portions of 0.1 N sodium hydroxide solution was added to each well to dissolve the protein and release the dye. The optical density of the resulting solution in each well was determined at 490 nm with a micro plate reader. The % inhibition of amoebal growth was calculated from the optical densities of the control and test wells and plotted against the logarithm of the dose of the drug tested. Linear regression analysis was used to determine the best fitting line from which the IC_{50} value was found.

5.2. In vitro antimalarial activity

The synthetic compounds, 4-14 were tested for their inhibitory effects on parasite growth by *in vitro* assay [37]. Various concentrations of each compound were obtained by 10-fold serial dilution in 96-well tissue culture plate. The control reaction was contained in 0.1% (v/v) final concentration of DMSO as a solvent without any compounds. Each concentration of compounds was tested in triplicate. The synchronized ring stage *P. falciparum* K1 strain was prepared from mixed stage parasite culture by 5% D-sorbitol treatment, the ring stage parasite was then mixed with culture medium containing RPMI 1640 supplemented with 10% human serum. The prepared parasite was distributed on each well containing 1% parasitemia and 2% hematocrit in a total volume of 100 µl. The reaction was incubated at 37°C in condition with 5% CO_2 for 72 hr, then frozen and kept at -20°C until measure the reaction.

The fluorescence intensity measurement based on the incorporation of SYBR Green fluorescence dye into dsDNA replicated during parasite growing was performed. Each plate was thawed at room temperature for 3 hr and culture samples in each well were gently mixed by pipetting. The 100 µl of mixed SYBR Green I (SYBR® Green I Nucleic Acid Gel Stain- 10,000X concentrate in DMSO, Invitrogen) with lysis buffer pH 7.5 containing 20 mM Tris, 5 mM EDTA, 0.008% (w/v) saponin and 0.08% (v/v) Triton X-100 was added into each well and incubate at room temperature for 1 hr. The fluorescence intensity was measured by Varioskan Flash Multimode Reader (Thermo Scientific, Vantaa, Finland) with excitation and emission wavelength of 485 and 535 nm, respectively. The percentage of fluorescence intensity of each compound concentration compared with control reaction without compound was representative of parasite amount. The standard curve of % fluorescence intensity and compound concentrations was generated and IC_{50} was analysed using SigmaPlot 12.0 software.

5.3. Cell viability (MTT) assay:

The compounds (5, 6, 8, 9, 10, 11, 12, MNZ and CQ) having less IC_{50} than metronidazole and chloroquine were subjected to the MTT assay. The compounds were dissolved in DMSO to 10 mM/ml and stored in freezer until use. Compounds were diluted to 100 µM/ml with culture medium and followed by 2-fold serial dilution with1% DMSO in medium. The Chinese hamster ovary (CHO) cells were obtained from NCCS (Pune, India). The cells were cultured in RPMI (Sigma) with 10% foetal bovine serum, 1% penicillin-streptomycin- Neomycin and incubated at 37 °C humidified incubator with 5% CO_2. The effect of compounds 5, 6, 8, 9, 10, 11, 12, the standard drug metronidazole (MNZ) and Chloroquinine (CQ) on cell proliferation was measured using an MTT-based assay [38]. Briefly, the cells (5,000/well) were incubated in triplicate in a 96-well plate in the presence of various concentrations of compounds 5, 6, 8, 9, 10, 11, 12, MNZ, CQ and vehicle (DMSO) alone in a final volume of 100µL at 37°C and 5% CO_2 in a humidified atmosphere chamber for 48 h. At the end of this time period, 20 µL of MTT solution (5 mg/mL in PBS) was added to each well, and the cells were incubated at 37°C in a humidified atmosphere chamber for 4 h. After 4 h, the supernatant was removed from each well. The coloured formazan crystal produced from MTT was dissolved in 100 µL of DMSO, and then the absorbance (A) value was measured at 570 nm by a multi-scanner auto reader. The following formula was used for the calculation of the percentage of cell viability (CV): CV (%) = (A of the experimental samples/A of the control) × 100.

5.4. ADMET Predictions

Discovery studio 3.5 (Accelrys San Diego, USA) was used to generate ADMET values. The Absorption, Distribution, Metabolism, Excretion and Toxicity commonly abbreviated as ADMET properties are considered before designing a drug as these properties play an important role in clinical phases. Administration of these properties before drug designing leads to cost savings in drug design [39]. These studies resulted in identification of anti-protozoal compounds. The after effects of drug intake are administered by TOPKAT. It assesses the toxicological endpoints by Quantitative Structure Toxicity Relationship (QSTR). Ames mutagen predication, Ames probability, Ames enrichment and weight of evidence were tested by toxicity profile of the compounds.

5.5. Molecular docking

Molecular docking in recent years has been recognised as a well-established computational technique for predicting the pose and interaction energy between receptor and ligand molecules [40-43]. The crystal structure of wild-type Plasmodium falciparum dihydrofolate reductase (PDB id: 1J3I) co-crystallized with the ligand (WR99210) was taken for docking [44]. To identify the key residues of *Pf*DHFR that interact with the thienopyrimidine sulphonamide hybrids (5, 6 and 8) we have used Autodock 4.2. Docking simulations were performed using Lamarckian Genetic algorithm (LGA). The grid maps representing the ligand were calculated with Autogrid. The dimensions of the grid were 40x40x40 grid points with a spacing of 0.375 Å between the grid points and centered on the ligand (27.71, 6.508 and 58.3 coordinates) [45]. Docking was performed by creating an initial population of 150 individuals, maximum number of evaluation 2,500,000, maximum number of generations default. 10 docking conformations (poses) were generated and the best docked conformation was selected based on the Autodock binding energy. For generating the 2D interaction plots depicting hydrogen and hydrophobic interactions between ligand-receptor complexes Ligplot+ was used [46].

5.6 PfDHFR marker interaction with ligands

Plasmodium falciparum Dihydrofolate reductase (*Pf*DHFR) interactions with three selected synthesized compounds (5, 6 and 8) were done by using dot blot method with slight modification [47]. The *Pf*DHFR protein was purchased from Sigma, to check the purity on 10% SDS-PAGE (Sodium dodecyl sulphate-Polyacrylamide gel electrophoresis) and examine the effect of compounds on *Pf*DHFR protein for binding affinity. BSA (1.0 µg), *Pf*DHFR enzyme and various concentration of compounds with standard drug chloroquinine was dot-blotted on pre-charged nitrocellulose membrane. It was incubated in blocking buffer which was prepared using 25 mM NaCl, 10 mM $MgCl_2$, 10 mM HEPES, 0.1 mM EDTA, 1 mM DTT, and 3 % BSA. The substrate (DNA stretch) was labelled at the 5'-end by using T4 polynucleotide kinase (NEB, England) with 1.85MBq of YP^{32} ATP and purified using sepharose 4B bead column (Pharmacia, Sweden). The membrane was first blocked and then incubated for 1 h in binding buffer at 37 ^{0}C. An additional recharged membrane was dot-blotted with rising concentrations of compounds (2.5-100µM) to check for loading of proteins (100nM). This membrane was probed with alkaline phosphatase conjugated anti-his HRP antibody (Sigma Chemical Co.) for 1 h at room temperature. After blocking in blocking buffer (1 % BSA in Tris-buffered saline), the blot was washed thrice (5minutes x3) with binding buffer and developed by DAB (3, 3'-Diaminobenzidine) hydrogen peroxide solution. In parallel experiment the other blot was already probed with DNA substrate and then exposed for autoradiography.

6. Conclusion

Thienopyrimidine bearing the piperazine sulphonamide skeleton were designed and synthesized as hybrid agent's pocessing enhanced antiprotozoal activity. 9, 10, 11 and 12 showed the most promising results against the HM1: IMSS strain of *E. histolytica* The most potent compounds against *P. falciparum* in cultures were 5 and 8 with IC_{50} less than 0.1 µM. Docking studies with *Pf*DHFR showed that the inhibitors place themselves nicely into the active site of the enzyme and revealed the interacting residues in the binding pocket. The result revealed that the compounds (5 and 6) bind to the enzyme properly and showed signal as compared to 8. The compounds 5 and 6 are the best compounds against *Pf*DHFR as compared to others. All these observations from *in-vitro* and *in-silico* studies suggest that compounds 5 and 6 are potent, which can be further studied for the development of novel pharmacophore against *Pf*DHFR.

Notes and references

[1] K. S. Ralston, W. A. Petri, *Essays Biochem.,* 2011, 51, 193.

[2] A. Bendesky, D. Menendez, P. Ostrosky-Wegman, *Mutat. Res.,* 2002, 11, 133.

[3] S. Becker, P. Hoffman, E. R. Houpt, *Am. J. Trop. Med. Hyg.,* 2011, 84, 581.

[4] World Health Organization, status 2014, http://www.who.int/malaria/media/world malaria report 2013/en/.

[5] I. Petersen, R. Eastman, M. Lanzer, *FEBS Letters,* 2011, 585, 1551.

[6] C. Viegas-Junior, A. Danuello, V. da S. Bolzani, E. J. Barreiro, C. A. M. Fraga, *Curr. Med. Chem.,* 2007, 14, 1829.

[7] L. K. Gediya, V. C. Nijar, *Expert Opin. Drug Discov.,* 2009, 4, 1099.

[8] N. Sharma, D. Mohanakrishnan, A. Shard, A. Sharma, Saima, A. K. Sinha, D. Sahal, *J. Med. Chem.,* 2011, 55, 297.

[9] S. Ananthan, E. R. Faaleolea, R. C. Goldman, J. V. Hobrath, C. D. Kwong, B. E. Laughon, J. A. Maddry, A. Mehta, L. Rasmussen, R. C. Reynolds, J. A. Secrist III, N. Shindo, D. N. Showe, M. I. Sosa, W. J. Suling, E. L. White, *Tuberculosis,* 2009, 89, 334.

[10] V. Alagarsamy, S. Vijayakumar, V. R. Solomon, *Biomed. Pharmacotherapy,* 2007, 61, 285.

[11] Y. D. Wang, S. Johnson, D. Powell, *Bioorg. Med. Chem. Lett.,* 2005, 15, 3763.

[12] T. Horiuchi, J. Chiba, K. Uoto, T. Soga, *Bioorg. Med. Chem. Lett.,* 2009, 19, 305.

[13] A. Cohena, P. Suzanneb, J. C. Lancelot, P. Verhaeghe, A. Lesnard, L. Basmaciyana, S. Huttera, M. Lageta, A. Dumetrea, L. Paloqued, E. Deharod, M. D. Crozete, P. Rathelote, P. Dallemagne, A. Lorthiois, C. H. Sibleyg, P. Vanellee, A. Valentin, D. Mazier, S. Rault, N. Azas, *Eur. J. Med. Chem.,* 2015, 95, 16.

[14] O. Donkor, H. Li, S. F. Queener, *Eur. J. Med. Chem.,* 2003, 38, 605.

[15] A.Gangjee, W. Li, R. L. Kisliuk, V. Cody, J. Pace, J.Piriano, J. Makin*, J. Med. Chem.,* 2009, 52, 4892.

[16] A. Gangjee, Y. Qiu, W. Li, R. L. Kisliuk, *J. Med. Chem.,* 2008, 51, 5789.

[17] L. Rong-Jian, A. T. John, Z. Tatiana, K. Olga, K. Vitalii, K. Svetlana, S. Sergey, P. Jason, T. Sagun, B. Enugurthi, Y. Yang, W. Jian, F. Stephanie, F. Shelly, S. Alana, Z. Jiying, S. O. Sherry, G. Michael, B. Dani, B. Brian, K. Barney, J. Peter, K. Alisher, M. You-An, J. Cynthia, L. Changhui, P. Tatiana, Z. Tong, C. Alexander, L. Rongshi, S. Connie, *J. Med. Chem.,* 2007, 50, 6535.

[18] J. N. N. S. Chandra, C. T. Sadashiva, C. V. Kavitha, K. S. Rangappa, *Bioorg. Med. Chem.,* 2006, 14, 6621.

[19] C. S. A. Kumar, S. B. B. Prasad, K. Vinaya, S. Chandrappa, N. R. Thimmegowda, Y. C. S. Kumar, S. Sanjay, K. S. Rangappa, *Eur. J. Med. Chem.,* 2009, 44, 1223.

[20] Z. Gang, C. T. Pauline, A. Robert, C. Jianhua, W. K. David, K. Rongze, F. L. Joe, S. John, W. Heping, R. J. Herr, J. Z. Andrew, Y. Jinhai, L. Sang, W. Samuel, A. B. Todd, M. M. Paul, X. Yiming, S. W. Scott, *Bioorg. Med. Chem. Lett.,* 2011, 21, 2890.

[21] X. Jason, W. Zhao-Kui, L. Huan-Qiu, I. Manus, B. Eva, N. Jill, C. Lihren, C. John, S. M. Tarek, X. Xin, S. Vipin, T. May, X. Yuzhe, L. Xiangping, H. Seung, T. James, S. Eddine, *J. Med. Chem.,* 2008, 51, 4068.

[22] K. P. Harish, K. N. Mohana, L. Mallesha, B. N. P. Kumar, *Eur. J. Med. Chem.,* 2013, 65, 276.

[23] S. Talath, A. K. Gadad, *Eur. J. Med. Chem.,* 2006, 41, 918.

[24] A. Salahuddin, A. Inam, R. L. van Zyl, D. C. Heslop, C. T. Chen, F. Avecilla, S. M. Agarwal, A. Azam, *Bioorg. Med. Chem.,* 2013, 21, 3080.

[25] C. Wu, M. S. Coumar, C. Chu, W. Lin, Y. Chen, C. Chen, H. Shiao, S. Rafi, S. Wang, H. Hsu, C. Chen, C. Chang, T. Chang, T. Lien, M. Fang, K. Yeh, C. Chen, T. Yeh, S. Hsieh, J. T. A. Hsu, C. Liao, Y. Chao, H. Hsieh, *J. Med. Chem.,* 2010, 53, 7316.

[26] H. Van De Waterbeemd, E. Gifford, *Drug discovery.* 2003, 2, 192.

[27] C. de Graaf, N.P. Vermeulen, K. A. Feenstra, *J. med. chem.* 2005, 48, 2725.

[28] V.Srimai, M.Ramesh, K.S. Parameshwar, T. Parthasarathy, *Med. Chem. Research.* 2013, 22, 5314.

[29] P. Singh, F. Bast, *Med. Chem.Research.* 2014, 23, 1690.

[30] H. Pajouhesh, G.R. Lenz,*NeuroRx.* 2005, 2, 541.

[31] SHELX, G. M. Sheldrick, Acta Crystallogr., Sect. A, 64 (2008) 112–122.

[32] G. M. Sheldrick, SADABS, version 2.10, University of Göttingen, Germany, (2004).

[33] C. W. Wright, M. J. O'Neill, J. D. Phillipson, D. C. Warhurst, *Antimicrob. Agents Chemother.,* 1988, 32, 1725.

[34] L. S. Diamond, D. R. Harlow, C. C. R. Cunnick, *Trans. R. Soc. Trop. Med. Hyg.,* 1978, 72, 431.

[35] F. D. Gillin, D. S. Reiner, M. Suffness, *Antimicrob. Agents Chemother.,* 1982, 22, 342.

[36] A. T. Keene, A. Harris, J. D. Phillipson, D. C. Warhurst, *Planta Med.,* 1986, 52, 278.

[37] M. A. Rason, T. Randriantsoa, H. Andrianantenaina, A. Ratsimbasoa, D. Menard, *Trans R. Soc. Trop. Med. Hyg.,* 2008, 102, 346.

[38] T. Mosmann, *J. Immunol Methods,* 1983, 65, 55.

[39] H.E. Selick, A.P. Bereford, M.H Tarbit, *Drug Discov Today.* 2002, 7, 109.

[40] M. F. Ansari, S. M. Siddiqui, S. M. Agarwal, K. S. Vikramdeo, N. Mondal, A. Azam, Bioorg. Med. Chem. Lett., 2015, 25, 3545.

[41] A. Salahuddin, S. M. Agarwal, F. Avecilla, A. Azam, *Bioorg. Med. Chem. Lett.,* 2012, 22, 5694.

[42] M. Y. Wani, F. Athar, A. Salauddin, S. M. Agarwal, A. Azam, I. Choi, A. R. Bhat, *Eur. J. Med. Chem.*, 2011, 46, 4742.

[43] I. S. Yadav, P. P. Nandekar, S. Shrivastava, A. Sangamwar, A. Chaudhury, S. M. Agarwal, *Gene*, 2014, 539, 82.

[44 J. Yuvaniyama, P. Chitnumsub, S. Kamchonwongpaisan, J. Vanichtanankul, W. Sirawaraporn, P. Taylor, M. D. Walkinshaw, Y. Yuthavong, *Nat. Struct. Biol.*, 2003, 10, 357.

[45] A. Inam, R. L. Van Zyl, N. J. van Vuuren, C. Chen, F. Avecilla, S. M. Agarwal, A. Azam, *RSC Adv.,* 2015, 5, 48368.

[46] R. A. Laskowski, M. B. Swindells, *J. Chem. Inf. Model.,* 2011, 51, 2778.

[47] E. C. B. Jr. Nadala, P. C. Loh, *J. Virol. Methods,* 2000, 175.

Caption to Illustration

Caption Heading

Figure 1 Design of hybrid compounds

Figure 2: ORTEP plot of the compound 4-[4-(Propane- 1- sulphonyl)- piperazine-1-yl] – 5,6,7,8- tetrahydrobenzo [4,5] theino [2,3-d] pyrimidine (9). All the non-hydrogen atoms are presented by their 50% probability ellipsoids. Hydrogen atoms are omitted for clarity.

Figure 3: ORTEP plot of the compound 4-[4-Benzenesulphonyl) – piperazine – 1 –yl] -5,6,7,8 –tetrahydro-benzo [4,5] theino [2,3 –d] pyrimidine (13). All the non-hydrogen atoms are presented by their 50% probability ellipsoids. Hydrogen atoms are omitted for clarity.

Figure 4: Atropoisomers *aR*- and *aS*- present in the crystal packing of compound 13.

Figure 5: Viability of CHO Normal cells in response to different compounds. Cells were plated in triplicates for 48 h and treated with the compounds. Cells treated with DMSO are used as the control.

Figure 6: Ligplot showing hydrogen bonding interaction and hydrophobic contacts (with green dashed lines and red arcs with radiating lines respectively) for the ligand (A) WR99210 (B) 5 (C) 6 and (D) 8.

Figure 7: Affinity binding activities on *Pf*DHFR. **A.** (Protein+compounds), **B.** (Protein+Substrtae), **C.** Lane 1-6 different concentration of compounds (a, c and e) and Scan result of PfDHFR with phosphor imager (b, d and f)

Scheme 1: Synthesis of 4-piperazin-1-yl-5,6,7,8-tetrahydrobenzo [4,5]theino[2,3-d] pyrimidine based sulphonamides.

Table 1: *In vitro* antiamoebic and antimalarial activity of thienopyrimidine sulphonamide hybrids against HM1: IMSS strain of *E. histolytica,* K1 strain of *P. falciparum*.

Table 2: Pharmacokinetics profile of known inhibitors and synthesize compounds

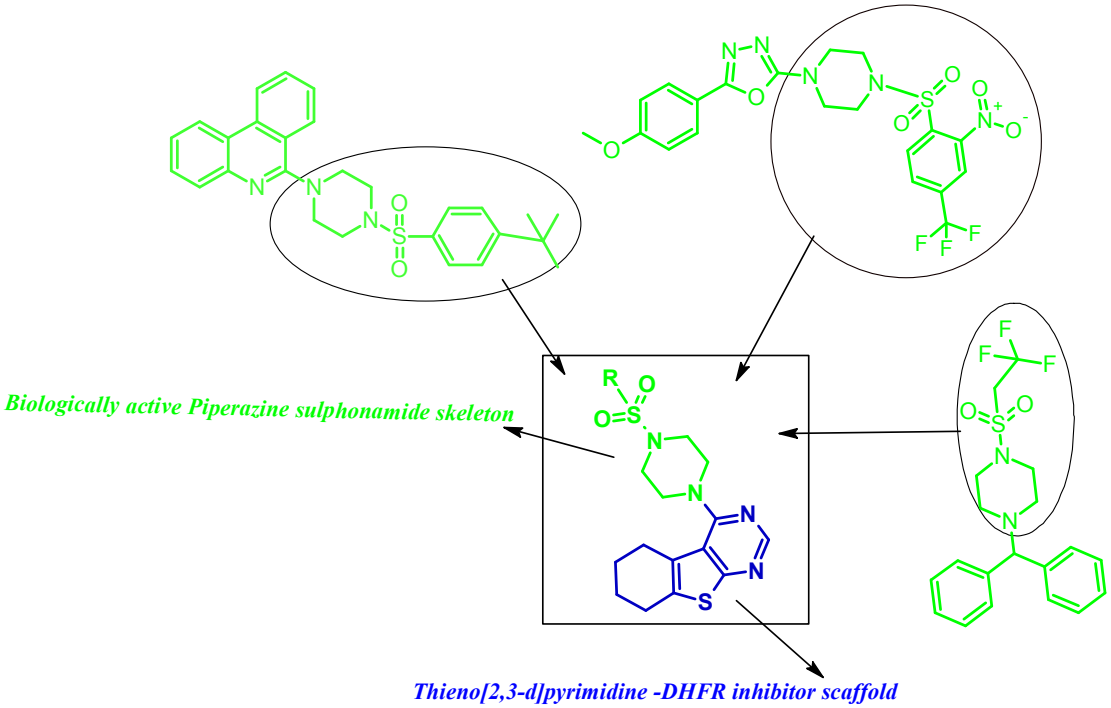

Figure 1: Design of hybrid compounds

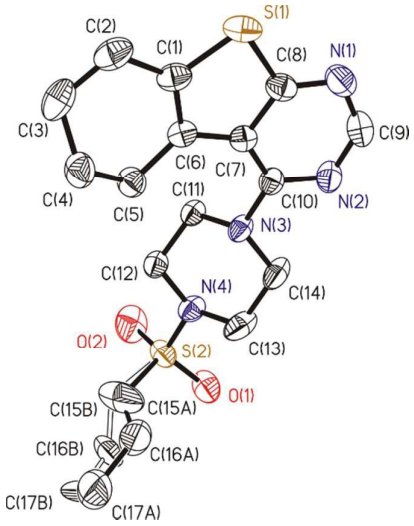

Figure 2: ORTEP plot of the compound 4-[4-(Propane- 1- sulphonyl)- piperazine-1-yl] – 5,6,7,8-tetrahydrobenzo [4,5] theino [2,3-d] pyrimidine (9). All the non-hydrogen atoms are presented by their 50% probability ellipsoids. Hydrogen atoms are omitted for clarity

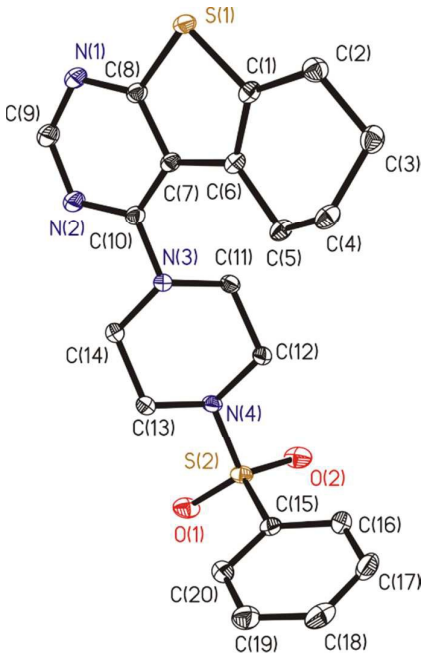

Figure 3: ORTEP plot of the compound 4-[4-Benzenesulphonyl) – piperazine – 1 –yl] -5,6,7,8 – tetrahydro-benzo [4,5] theino [2,3 –d] pyrimidine (13). All the non-hydrogen atoms are presented by their 50% probability ellipsoids. Hydrogen atoms are omitted for clarity.

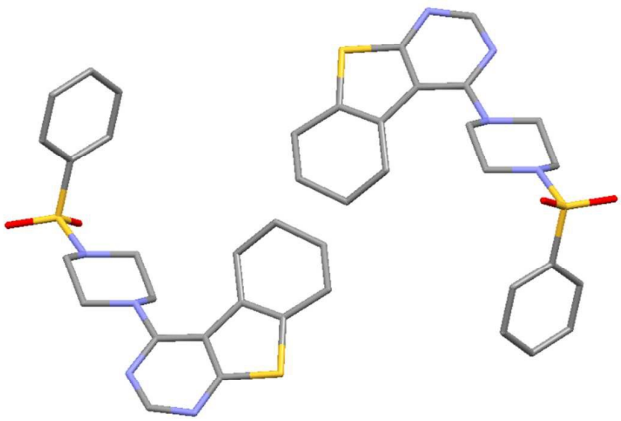

Figure 4: Atropoisomers *aR*- and *aS*- present in the crystal packing of compound 13.

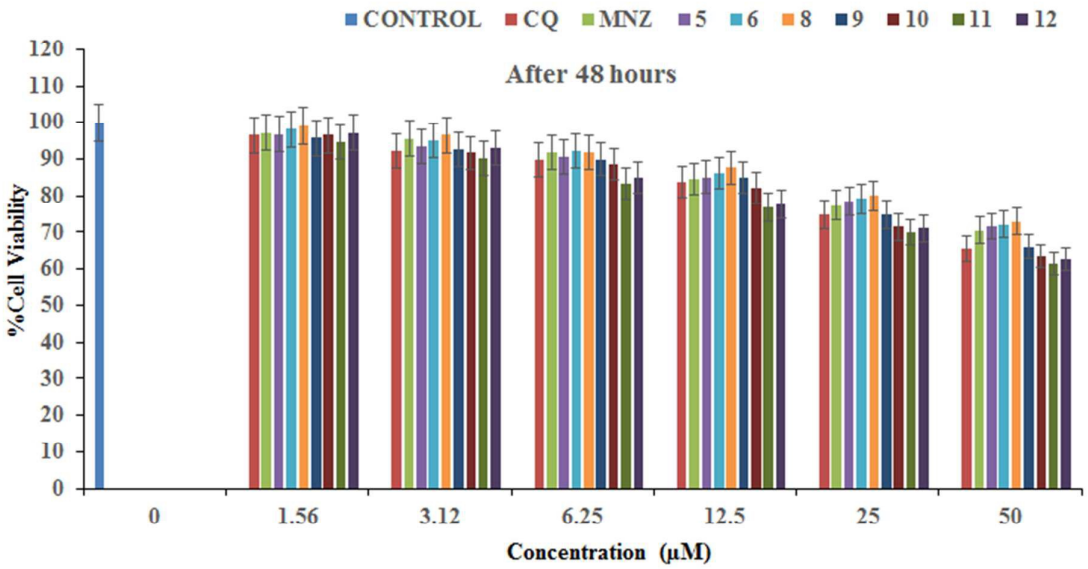

Figure 5: Viability of CHO Normal cells in response to different compounds. Cells were plated in triplicates for 48 h and treated with the compounds. Cells treated with DMSO are used as the control.

.

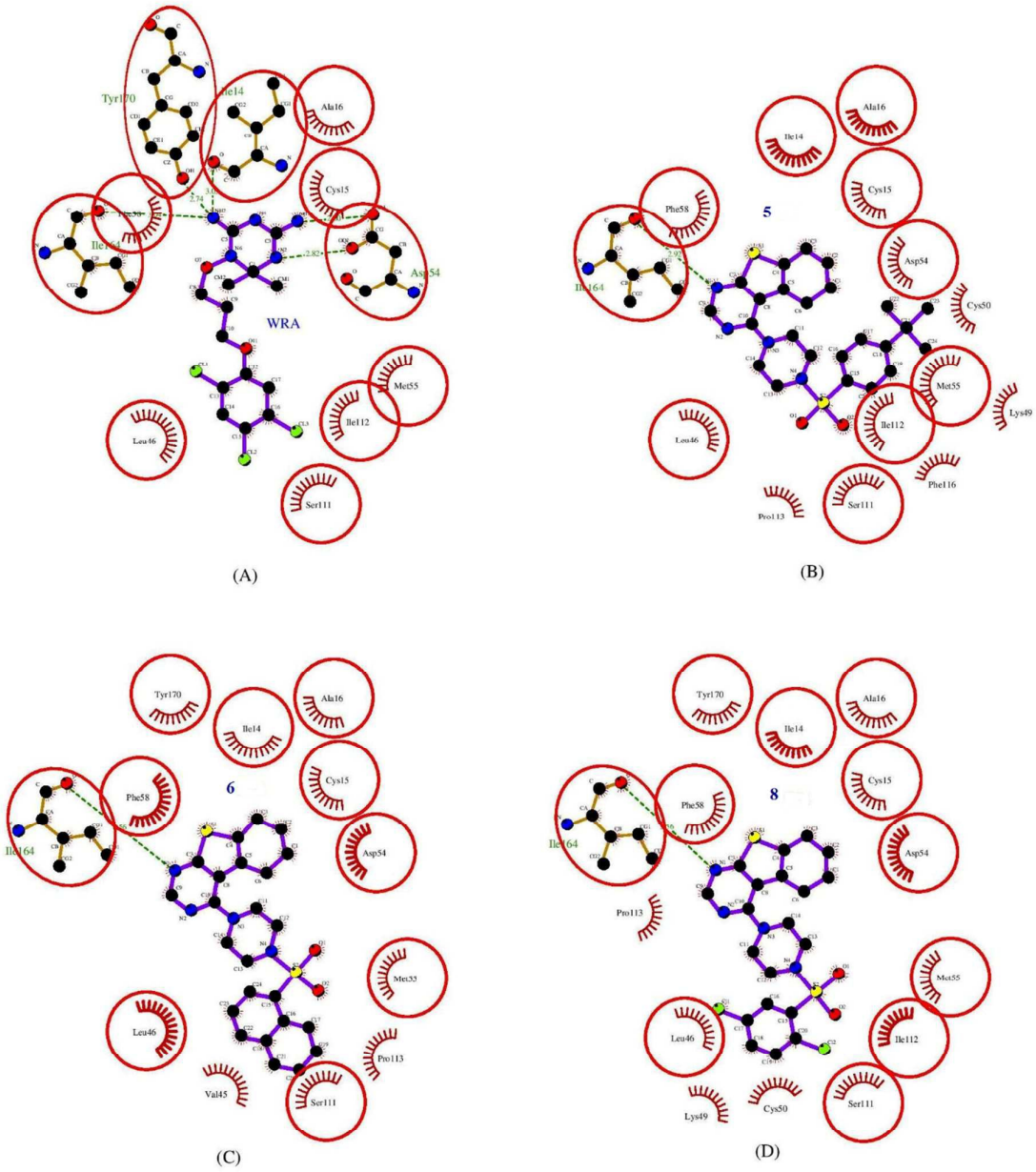

Figure 6. Ligplot showing hydrogen bonding interaction and hydrophobic contacts (with green dashed lines and red arcs with radiating lines respectively) for the ligand (A) WR99210 (B) 5 (C) 6 and (D) 8.

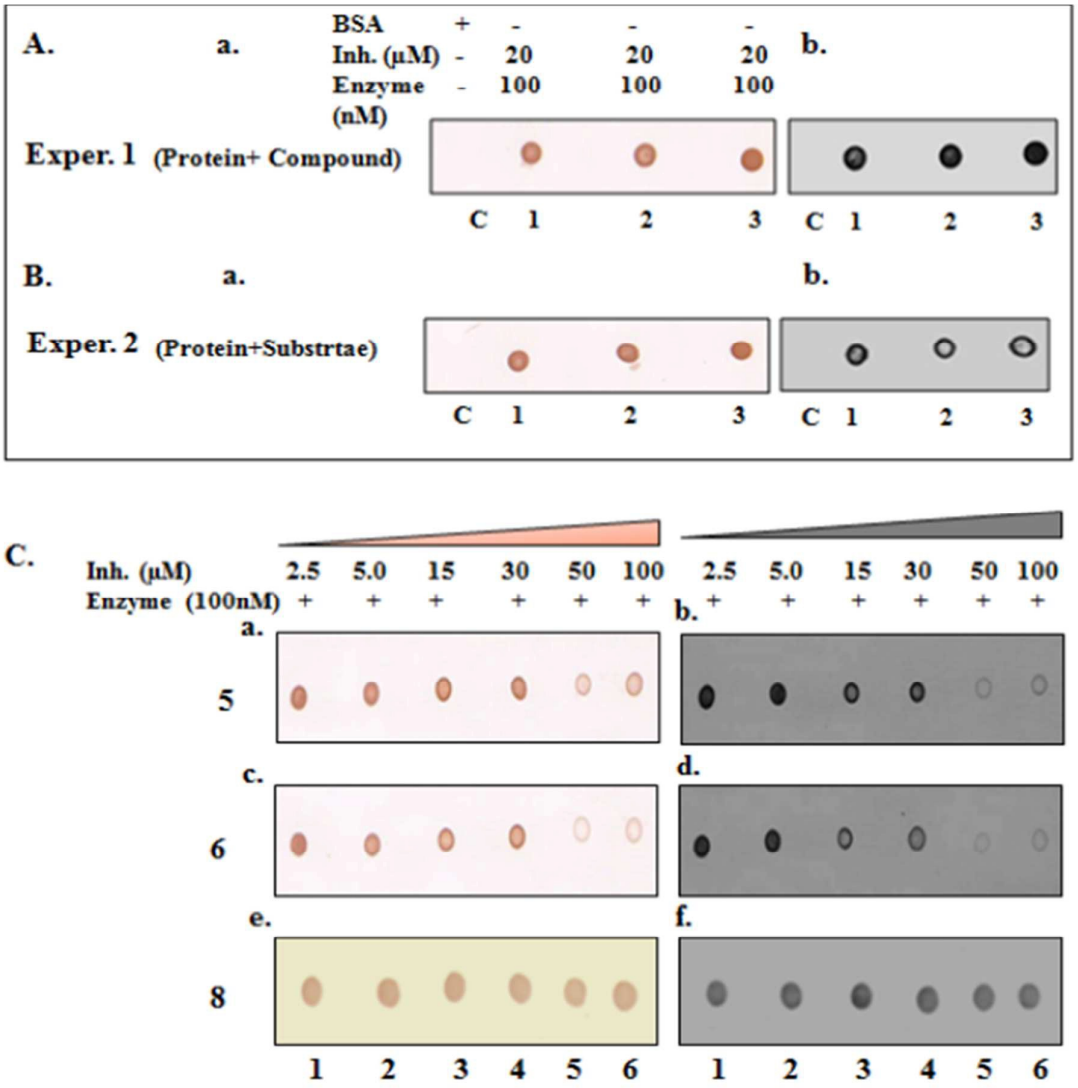

Figure 7: Affinity binding activities on *Pf*DHFR. **A.** (Protein+compounds), **B.** (Protein+Substrtae), **C.** Lane 1-6 different concentration of compounds (a, c and e) and Scan result of PfDHFR with phosphor imager (b,d and f)

Scheme 1: Synthesis of 4-piperazin-1-yl-5,6,7,8-tetrahydrobenzo [4,5]theino[2,3-d] pyrimidine based sulphonamides.

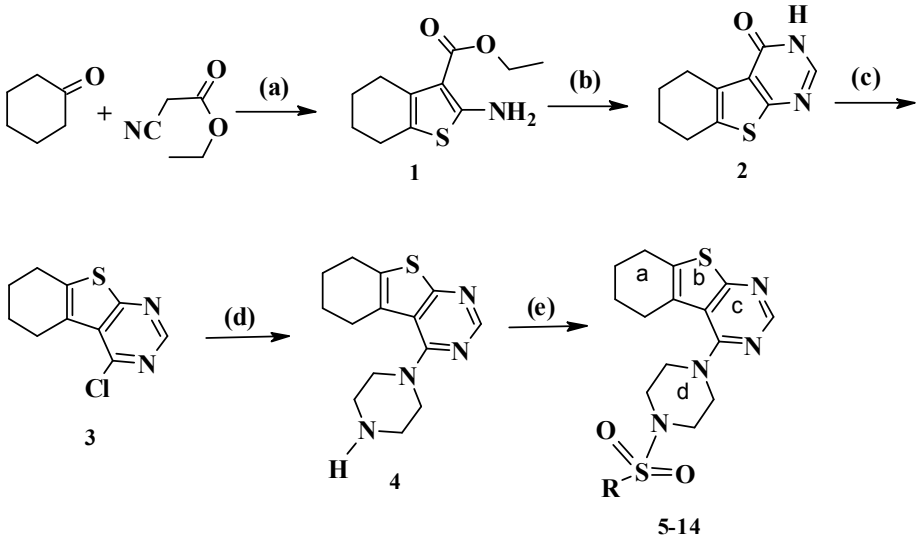

Where R = 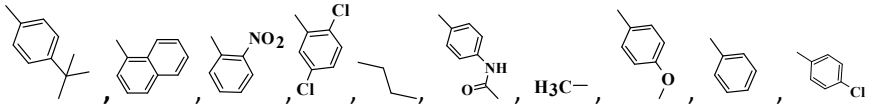

Reagents and conditions: *(a) S_8, Et_3N, EtOH (b) formamide, reflux (c) $POCl_3$, reflux (d) piperazine, EtOH (e) R-sulphonyl chloride, Et_3N, DCM*

Table 1: *In vitro* antiamoebic and antimalarial activity of thienopyrimidine sulphonamide hybrids against HM1: IMSS strain of *E. histolytica,* K1 strain of *P. falciparum*.

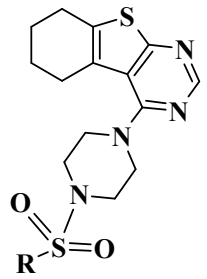

Compound Code	R	Antiamoebic **(IC_{50}±S.D)** (μM)	Antimalarial **(IC_{50}±S.D)** (μM)	Cytotoxicity **(IC_{50}±S.D)** (μM)
4		3.29±0.02	2.07±0.01	N.D.[c]
5	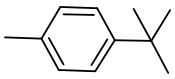	5.8±0.02	<0.1	> 50 μM
6	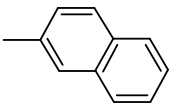	4.6±0.01	0.1±0.001	> 50 μM
7	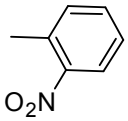	3.0±0.02	7.85±0.02	N.D.
8	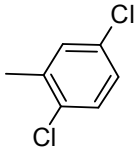	2.82±0.02	<0.1	> 50 μM
9		1.36±0.01	1.02±0.01	> 50 μM
10	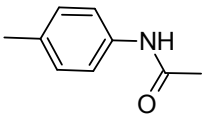	0.78±0.01	1.98±0.01	> 50 μM
11	CH_3	1.70±0.01	0.9±0.001	> 50 μM
12	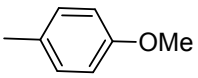	0.35±0.03	1.94±0.02	> 50 μM
13	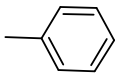	4.13±0.02	3.15±0.02	N.D.
14	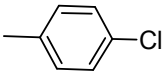	2.02±0.02	18.5±0.03	N.D.
Metronidazole		1.86±0.02		> 50 μM
Chloroquine			0.42±0.02	> 50 μM

[a] The values obtained in at least three separate assays done in triplicate
[b] Standard Deviation [c] Not Done

Table 2: Pharmacokinetics profile of known inhibitors and synthesize compounds

ADMET											TOPKAT		
Compound no.	**BBB**	**AlogP**	**Sol.**	**HIA**	**HTL**	**HT_ Prob**	**PPB**	**CYP2D6**	**PSA**	**Ames Mut.**	**Prob**	**Enrichment**	**WOE**
Synthesize molecules													
5	1	5.348	1	0	0	0.34	2	0	63.82	NM	0.27	0.48	NC
6	1	4.856	1	0	0	0.17	1	0	63.82	NM	0.62	1.12	NC
8	1	5.277	1	0	0	0.41	2	0	63.82	NM	0.41	0.74	NC
Known Inhibitors													
Chloroquine	3	0.029	4	0	0	0.33	0	0	42.55	NM	0.15	0.28	C

BBB: Blood Brain Barrier Level 0-4, having high penetration to no penetration, **HIA:** Human Intestinal Absorption level ideal value range from 0-1 as good to moderate, **Sol**. (Solubility Level): Ideal value of solubility level is 3, **HTL:** Hepatotoxicity level ideal value range from 0-1 as good to moderate, **HT- Prob.:** Hepatotoxicity probability <0.5 is ideal, **CYP2D6**<0.5 is good and denoted with level 0, **PPB:** Plasma protein binding value 0 is good and compounds to accessible with BBB, **AlogP** value should not be greater than 5.0 and polar surface area ≤ 140 is ideal. **Ames Mut:** Ames mutagen prediction, **Prob.:** Ames probability; Enrichment: Ames enrichment; **WOE-_Prediction** (weight of evidence); M: (Mutagen); NM: (Non-Mutagen); C: (Carcinogen); NC: (Non-Carcinogen).

Thienopyrimidine sulphonamide hybrids: Design, synthesis, antiprotozoal activity and molecular docking studies

Saadia Leeza Zaidi[a], Subhash M Agarwal[b], Porntip Chavalitshewinkoon-Petmitr[c], Thidarat Suksangpleng[c], Kamal Ahmad[d]Fernando Avecilla[e] , Amir Azam[a*]

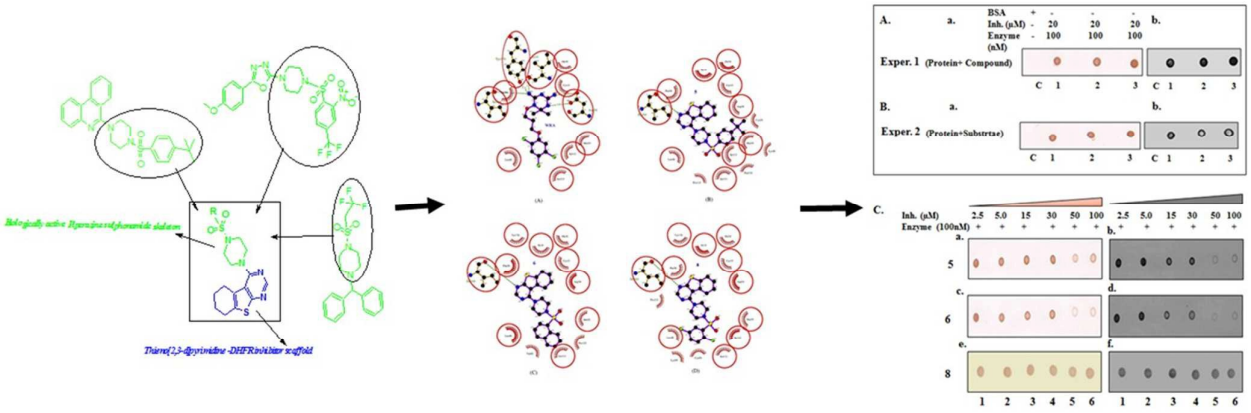

Designing Docking on *Pf*DHFR Affinity binding activities on *Pf*DHFR